Available online at www.sciencedirect.com
SCIENCE DIRECT
International Journal of Heat and Mass Transfer 49 (2006) 2458–2465
International Journal of HEAT and MASS TRANSFER
www.elsevier.com/locate/ijhmt

Generalized neural network correlation for flow boiling heat transfer of R22 and its alternative refrigerants inside horizontal smooth tubes

Wei-Juan Wang [a], Ling-Xiao Zhao [a], Chun-Lu Zhang [b,*]

[a] Institute of Refrigeration and Cryogenics, Shanghai Jiaotong University, Shanghai 200030, China
[b] China R&D Center, Carrier Corporation, #29-06 King Tower, No. 28 Xinjinqiao Road, Pudong, Shanghai 201206, China

Received 12 August 2004; received in revised form 15 April 2005
Available online 23 March 2006

Abstract

The correct prediction of refrigerant boiling heat transfer performance is important for the design of evaporators. A generalized neural network correlation for boiling heat transfer coefficient of R22 and its alternative refrigerants R134a, R407C and R410A inside horizontal smooth tubes has been developed in this paper. Four kinds of dimensionless parameter groups from existing generalized correlations are selected as the input of neural network, while the Nusselt number is used as the output. Three-layer perceptron is employed as the universal approximator to build the relationship between the input and output parameters. The neuron number of hidden layer is determined by the performance of model accuracy and the standard sensitivity analysis. The experimental data of the four refrigerants in open literatures are used for correlation. The results show that the input parameter group based on the Gungor–Winterton correlation is better than the other three groups. Compared with the experimental data, the average, mean and root-mean-square deviations of the trained neural network are 2.5%, 13.0% and 20.3%, respectively, and approximately 74% of the deviations are within ±20%, which is much better than that of the existing generalized correlations.

Keywords: Boiling heat transfer; Horizontal smooth tube; Refrigerant; Neural network

1. Introduction

CFC (chlorofluorocarbon) and HCFC (hydrochlorofluorocarbon) refrigerants cause global warming and ozone depletion, bring on the environmental problems. So, UN drew up the Montreal Protocol and its London and Copenhagen Amendments [1,2], raising a clear schedule to forbid the production and usage of CFC and HCFC. According to the Montreal Protocol, R22 which has been widely used in air conditioners will be discarded completely in 2020. So the development of new alternative refrigerants and prompt shift to new refrigerants are mostly required to protect the environment. A lot of researches have been done to find the alternative refrigerants in the past 15 years. Now, in air-conditioning field R410A, R407C and R134a are looked as the alternative refrigerants of R22, which are applied to different refrigerating system with a gradually increasing refrigerating capacity, respectively.

The importance of correctly predicting saturated flow boiling heat transfer coefficients has been well recognized, as seen from a large number of analytical and experimental investigations conducted in the past years [3,4]. Knowledge of these coefficients can reduce the cost and avoid the drastic results due to under-design or over-design evaporators. There are a large number of saturated flow boiling correlations available in the literature. The flow boiling correlation in general can be classified into two categories. Under the first category, the correlations are developed by experimental investigators to represent their own data [5,11,19]. After ascertaining the accuracy of the experiments conducted, these individual correlations can be used by the user within the same range of parameters. The

* Corresponding author. Tel.: +86 21 5030 7806; fax: +86 21 5030 7807.
E-mail address: chunlu.zhang@carrier.utc.com (C.-L. Zhang).

0017-9310/$ - see front matter © 2006 Elsevier Ltd. All rights reserved.
doi:10.1016/j.ijheatmasstransfer.2005.12.021

Nomenclature

Bo	Boiling number, $q/(G \cdot i_{fg})$
Co	Convection number, $((1-x)/x)^{0.8}\ (\rho_g/\rho_l)^{0.5}$
c_p	specific heat (J kg^{-1} K^{-1})
D	tube diameter (m)
Fr_l	Froude number, $G^2/(\rho_l^2 gD)$
G	mass flow rate (kg m^{-2} s^{-1})
g	acceleration of gravity (m s^{-2})
h	heat transfer coefficient (W m^{-2} K^{-1})
i_{fg}	latent heat of vaporization (J/kg)
k	thermal conductivity (W m^{-1} K^{-1})
M	molecular weight
n	output neuron
Nu	Nusselt number, hD/k_l
p	pressure (Pa)
Pr	Prandtl number, $c_p\mu/k$
q	heat flux (W m^{-2})
Re_l	Reynolds number, $GD(1-x)/\mu_l$
T	temperature (°C)
u	weights between input later and hidden layer
w	weights between hidden layer and output layer
x	quality

Greek symbols

X_{tt}	Martinelli number, $((1-x)/x)^{0.9}(\rho_g/\rho_l)^{0.5}(\mu_l/\mu_g)^{0.1}$
μ	dynamic viscosity (N s m^{-2})
ρ	density (kg m^{-3})

Subscripts

fg	latent heat
g	gas
l	liquid
line	pure line transfer function
log	log-sig transfer function
meas	measurement
pred	predict
r	reduced parameter
sat	saturated
tan	tan-sig transfer function
tp	two phase

correlations under the second category are developed on the basis of a large number of data sets from different sources involving different fluids over a wide range of parameters [6–10]. These correlations are more valuable since they represent a large data base and cover a much broader range of operating conditions.

Table 1 gives five important correlations available in the literature. They are all based on a large number of data sets, and can represent the coefficients of different fluids and wide range of operating conditions. They have been used widely. However, there still exist some insufficiencies. Firstly, few of correlations involve all the above-mentioned four refrigerants in their data sets, especially for R410A and R407C. In addition to the correlations developed early, Choi et al. [11] proposed a correlation based on their own data involving R22, R134a, and R407C. This correlation shows a good result with their own data, but when compared to the data from other literatures it cannot give such good result. Secondly, the correlations reported in the literature have different function forms, which lack sufficient theoretical supports. When the two-phase flow boiling is considered, such simple correlation function cannot well reflect the complicated nonlinear relationship between the variables in a wide range of operating conditions.

Recently, some researchers used the artificial neural networks (ANNs) to correlate heat transfer coefficient [12–15], and got much better results than the traditional approach. The recent development of powerful learning algorithms

Table 1
Some popular generalized correlations for boiling heat transfer inside smooth tube

Literature	Fluids	Correlation
Liu and Winterton [6]	Water, R12, R22, R11, R113, R114, ethylene glycol, alcohol	$h_{tp}^2 = (Fh_{\text{Dittus–Boelter}})^2 + (Sh_{\text{Cooper}})^2, F = \left[1 + xPr_l\left(\frac{\rho_l}{\rho_g} - 1\right)\right]^{0.35}$, $S = (1 + 0.055F^{0.1}Re_l^{0.16})^{-1}, h_{\text{Dittus–Boelter}} = 0.023(k_l/D)Re_l^{0.8}Pr_l^{0.4}$, $h_{\text{Cooper}} = 55P_r^{0.12}q^{2/3}(-\log_{10}P_r)^{-0.55}M^{-0.5}$
Gungor and Winterton [8]	Water, R12, R22, R11, R113, R114, ethylene glycol, alcohol	$h_{tp} = Fh_{\text{Dittus–Boelter}} + Sh_{\text{Cooper}}, F = 1 + 24,000Bo^{1.16} + 1.37(1/X_{tt})^{0.86}$, $S = \frac{1}{1+1.15\times10^{-6}F^2Re_l^{1.17}}$, $h_{\text{Dittus–Boelter}}$ and h_{Cooper} are same as above
Jung and Radermacher [7]	R12, R22, R152a, R500, R114	$h_{tp} = Nh_{SA} + Fh_{\text{Dittus–Boelter}}, N = 4048X_{tt}^{1.22}Bo^{0.13}, F = 2.37\left(0.29 + \frac{1}{X_{tt}}\right)$, $h_{SA} = 207\frac{k_l}{bd}\left(\frac{qbd}{k_lT_{sat}}\right)^{0.745}\left(\frac{\rho_g}{\rho_l}\right)Pr_l^{0.533}$, where, $bd = 0.0146\beta[2\sigma/(g(\rho_l - \rho_v))]$, $h_{\text{Dittus–Boelter}}$ is same as above
Kandlikar [9]	Water, R11, R12, R22, R113, R114, R152, nitrogen	$\frac{h_{tp}}{h_{\text{Dittus–Boelter}}} = C_1Co^{C_2}(25Fr_l)^{C_5} + C_3Bo^{C4}F_{fl}$, where, $C1$–$C5$ and F_{fl} are seen in [10], $h_{\text{Dittus–Boelter}}$ is same as above
Shah [10]	Water, R11, R12, R22, R113, cyclohexane	$\frac{h_{tp}}{h_{\text{Dittus–Boelter}}} = f(Co, Bo, Fr_l)$

for the ANNs has led to their use in many engineering applications and the ANN has been an important tool to describe complicated problems. But all of them aimed at the special problems and used their own measured result as data sets, which led to some limitations in application. Furthermore, most of them directly used physical variables as the input of the ANNs, which could lead to high dimensionality and low generalization of the ANNs.

In this paper, owing to the good potential of the ANNs in approximation, the authors employ the ANNs as the correlation functions instead of the traditional ones to correlate the boiling heat transfer coefficients of R22, R410A, R407C and R134a flowing inside the horizontal smooth tubes. In the meantime, for the purpose of reducing the dimensionality and improving generalization of the ANNs, the input of ANNs consists of dimensionless parameters extracted from some existing generalized correlations. The data sets come from the open literatures [11,16–26,33] and comprise 1307 data.

2. Application of ANNs to in-tube flow boiling heat transfer

2.1. Basic principle of ANN

A neural network consists of a large number of simple processing elements called neurons or nodes. Each neuron is connected to other neurons by means of direct communication links with associated weights. The weights represent information being used by the network to solve a problem [27]. Among the various types of ANNs at present, the multilayer perceptron (MLP) has become the most popular in engineering applications [28,29]. There also are some other kinds of ANNs, such as radial basis function (RBF) and generalized regression neural network (GRNN). Generally, RBF and GRNN need more weights than MLP to obtain the same accuracy. In fact, we compared RBF, GRNN, and MLP in this case. The comparison showed the MLP is better than the other two. Therefore, for brevity, only MLP is discussed in this paper.

The network is simple in structure and easily analyzed mathematically. A typical three-layer perceptron is schematically illustrated in Fig. 1. This configuration has one input layer, one hidden layer and one output layer, whose numbers of neurons are I, J, K, respectively. Each neuron in input layer makes the weighted summation of all the neurons in the hidden layer, and then passes this summation through a transfer function. Next, the neuron in hidden layer makes the weighted summation of all the neurons in the output layer, and then passes the summation through the transfer function, which is the last output.

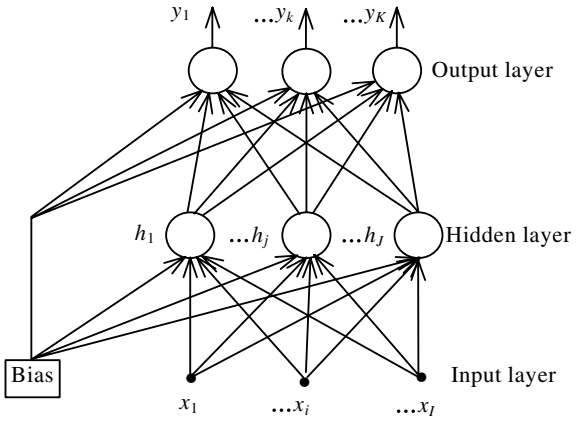

Fig. 1. Architecture of three-layer perceptron network.

To describe such relationship of input layer-hidden layer-output layer in mathematical form is as follows:

$$h_j = g\left(\sum_{i=0}^{I} u_{ji}x_i\right) \quad (j = 1,\ldots,J) \tag{1}$$

$$y_k = g\left(\sum_{j=0}^{J} w_{kj}h_j\right) \quad (k = 1,\ldots,K) \tag{2}$$

where, u_{ji} $(i > 0)$ is the associated weight connected by the ith neuron of input layer to the jth neuron of hidden layer. u_{j0} is the bias of the jth neuron of hidden layer. w_{kj} $(j > 0)$ is the associated weight connected by the jth neuron of hidden layer to the kth neuron of output layer. w_{k0} is the bias of the kth neuron of output layer.

2.2. ANNs used in this work

2.2.1. Input and output

To train and test the neural networks, input data patterns and corresponding targets were required. The object of this study is the flow boiling heat transfer, so we select heat transfer coefficient to be the output. To realize the universal application, Nusselt number is selected to be the output of ANNs.

The input of ANNs is based on the characteristic of the object we studied. Here we select the input based on the basic function form of five generalized correlations listed in Table 1. Table 2 lists the different input combination of ANNs based on different correlations, respectively.

In this study, three kinds of transfer function will be tried: log-sigmoid, tan-sigmoid, and pure linear, given in Eqs. (3)–(5).

$$g_{\log}(x) = 1/(1 + e^{-x}) \tag{3}$$

$$g_{\tan}(x) = 2/(1 + e^{-2x}) - 1 \tag{4}$$

$$g_{\text{line}}(x) = x \tag{5}$$

According to the log-sig and tan-sig transfer function defined by Eqs. (3) and (4), the output should be normalized within the interval $(0, 1)$ and $(-1, 1)$, respectively, and pure line function does not need normalized output. For the convenience of calculation, we normalize the output within the interval $(0, 1)$ to meet each transfer function's requirements by multiplying a little value constant to the original output parameter. In this study, the multiplier is 0.001. When the training completes, the corresponding denormalization should be done in prediction. The reciprocal of the

Table 2
Selection of the ANN input according to the generalized correlations in Table 1

Type	Dimensionless input parameters	Correlation
I	$Nu_{\text{Dittus–Boelter}}$, Nu_{Cooper}, $1 + xPr_l(\rho_l/\rho_g - 1)$, Re_l	Liu–Winterton [6]
II	$Nu_{\text{Dittus–Boelter}}$, $Nu_{\text{Stephan–Abdelsalam}}$, Bo, X_{tt}	Jung–Radermacher [7]
III	$Nu_{\text{Dittus–Boelter}}$, Nu_{Cooper}, Bo, X_{tt}	Gungor–Winterton [8]
IV	$Nu_{\text{Dittus–Boelter}}$, Bo, Co, Fr_l	Kandlikar [9] and Shah [10]

multiplier used in output normalization will be multiplied to the ANN predicted output to get the real value.

In addition, although the value of the ANN input is unlimited in terms of log-sig or tan-sig transfer function, if the absolute value of the input is very large, the output of hidden neuron will be very close to 0 or 1 and not sensitive to the input. Therefore, for the purpose of effective training, the input is also commonly normalized within or around the interval $(0, 1)$ or $(-1, 1)$ in the training step. For the convenience of using the trained ANN without repetitious normalization and denormalization, the input parameters can be normalized within or around the interval $(0, 1)$ by multiplying some positive constants. After the training step, the denormalization can be directly done by multiplying the weights between the input and hidden layers by those positive constants used in normalization. As a result, the real values of input can be straight used for a trained ANN. For the output, the normalization is also needed.

2.2.2. Number of hidden layer and hidden neurons

The capability of three-layer perceptron network to approximate any continuous function has been proved [30,31]. Furthermore, the more number of hidden layers, the more error transfer steps, which led to the decrease of the generalization. So this study firstly considers three-layer perceptron networks (one hidden layer).

The number of neurons in the hidden layer has to be found by balancing the model accuracy and the standard sensitivity. In the present case, the optimal value is found to be eight. The details will be given in the next section.

2.2.3. Training and test data

In developing an ANN model, the available data sets is divided into two parts, one to be used for training of the network (about 80% of the data), and the rest for testing the performance [32]. This study employs experimental data from the open literature, the details listed in Table 3. The total number of data sets is 1307, where 75% or 981 of the data randomly selected for training and the rest 25% data for test.

2.2.4. Training algorithm

In this study, we perform the calculation on the commercial software MATLAB 7.0. For the MLP network (in MATLAB, also called BP network), there are a dozen of training algorithms. By comparison, TRAINBR is found the best training algorithm in this case. Details about the algorithm can be seen in the help files of MATLAB 7.0.

In addition, there are three conditions at which iteration will end: (a) Training error reaches the expected value such as 0.001. (b) Gradient reaches the minimal value. (c) Number of iteration reaches the set value such as 20,000. ANN

Table 3
Data sources in the work

Refrigerant	Literature	D (mm)	G (kg/m^2 s)	q (kW/m^2)	T_{sat} (°C)	Number of data
R22	[16]	6.5	100–400	2.5–20	2	40
R22	[17]	7/9.52	70–211	5–15	−15 to 5	35
R22	[18]	9.52	224	10.85	5	4
R22	[11]	9.55	427	20.9	−2.9 to 5.9	69
R22	[21]	9.52	100–300	6–14	$p_{sat} = 0.6$ MPa	42
R22	[22]	10.7	150–300	10–30	14.15	238
R22	[25]	7.7	424–742	10–30	12	76
R22	[26]	9.52	311	28	27	14
R134a	[19]	10.92	300	5–20	5	106
R134a	[20]	6	250	10	20	8
R134a	[24]	7.7	424–583	30	12	19
R407C	[11]	9.55	427	20.9	−5.9 to 15.8	104
R407C	[16]	9.52	100–300	6–14	$p_{sat} = 0.6$ MPa	36
R407C	[20]	6	250	10	20	8
R407C	[23]	7	300	7.5	$p_{sat} = 0.545$ MPa	4
R407C	[25]	10.7	150–300	10–30	9.76	303
R410A	[22]	7, 9.52	70–211	5–15	−15 to 5	67
R410A	[24]	7.7	583	30	12	11
R410A	[23]	7	300	7.5	$p_{sat} = 0.545$ MPa	4
R410A	[33]	6	363–1098	11.6–38.5	−14.9 to 14.3	119

Table 4
Results of different transfer functions in hidden layer and output layer

Output layer	Hidden layer					
	Log-sig		Tan-sig		Pure line	
	Model accuracy RD (%)	Standard sensitivity RD (%)	Model accuracy RD (%)	Standard sensitivity RD (%)	Model accuracy RD (%)	Standard sensitivity RD (%)
Log-sig	22.0	4.8	21.8	5.9	35.7	2.0
Tan-sig	21.9	5.4	21.8	7.8	33.0	2.3
Pure line	21.6	10.0	22.9	11.3	33.9	2.2

model with log-sig and tan-sig transfer function always get result after hundreds iterations but that with pure line transfer function always ends up with 20,000 iterations.

2.2.5. Transfer function

There are three kinds of popular transfer functions can be used in BP network: log-sig, tan-sig, and pure line. ANN models with hidden and output layer using different combinations of the three transfer functions are tried. In the present case, we choose log-sig and log-sig combination as our model's hidden and output transfer function by comparing each model's accuracy and standard sensitivity. More details will be given in next section.

3. Results and discussions

3.1. General results

To find a good model, the standard sensitivity analysis is recommended [34]. We choose 15 sets of data among the total 1307 test data, give each input of the 15 points 50 disturbances using Gaussian error of $\sigma = 5\%$ with zero mean to see the difference between the ANN predicted result using Gaussian error input and that using original input. This difference is called the standard sensitivity. If the root mean deviation result of the standard sensitivity is around 5%, it means a good standard sensitivity is reached. Here, we tried three transfer functions in BP network's hidden and output layer: log-sig, tan-sig, and pure line. Table 4 gives the result based on the input type I. When pure line is used in both hidden and output layer, ANN model shows a good standard sensitivity but a poor accuracy and long time was taken in convergence. If pure line was not used in hidden layer, ANN models with all three transfer function combinations show a similar accuracy, but those who use pure line as output transfer function show a poor standard sensitivity. In addition, ANN models using log-sig or tan-sig transfer functions in the hidden and the output layers show a similar accuracy and standard sensitivity, but when using the model with tan-sig output transfer function, it is not easy to catch a result with both good accuracy and standard sensitivity in the calculation process. So in the following calculation, we employed log-sig and log-sig combination as hidden and output layer transfer function.

To find out the optimal number of hidden neurons, we also use the standard sensitivity analysis. Fig. 2 gives the ANN model accuracy and the standard sensitivity analysis result using combination III. From the figure we can see, the ANN model accuracy increased with the increased neuron number of hidden layer, but the standard sensitivity became worse. Balancing the accuracy and the sensitivity, we recommend the ANN model with 8 hidden neurons as the optimal model under the combination III. Similar procedure is repeated to find out the optimal hidden neuron numbers of the ANN models with type I, II, and IV of inputs, respectively.

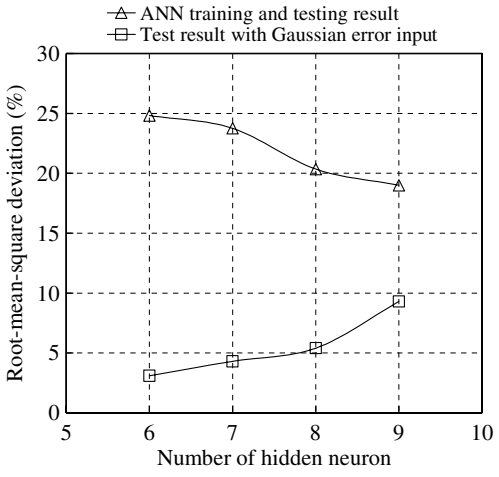

Fig. 2. Root-mean-square deviation versus number of hidden neuron (input type III).

Table 5
Comparison of ANN with different type of input

Deviation (%)	Type I		Type II		Type III		Type IV	
	Training	Test	Training	Test	Training	Test	Training	Test
AD	3.1	2.5	4.7	4.9	2.6	2.0	3.5	3.7
MD	15.2	14.9	18.3	19.0	12.9	13.2	17.3	18.5
RD	21.2	20.9	25.6	26.8	20.1	21.1	25.8	26.6

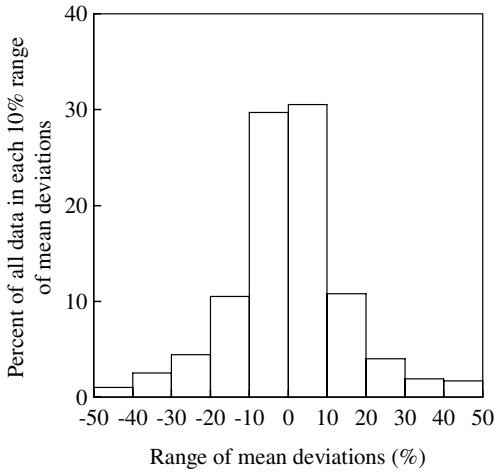

Fig. 3. Histogram of mean deviation for all data with the optimal ANN.

Table 5 shows the comparison of optimized ANN models with different type of input, where the average deviation (AD), mean deviation (MD), and root-mean-square of deviation (RD) are defined as follows:

$$\text{Average deviation} = \frac{1}{N}\sum_{N}[(h_{\text{pred}} - h_{\text{meas}})/h_{\text{meas}}] \times 100\% \quad (6)$$

$$\text{Mean deviation} = \frac{1}{N}\sum_{N}|(h_{\text{pred}} - h_{\text{meas}})/h_{\text{meas}}| \times 100\% \quad (7)$$

Root-mean-square deviation

$$= \sqrt{\frac{1}{N}\sum_{N}[(h_{\text{pred}} - h_{\text{meas}})/h_{\text{meas}}]^2} \times 100\% \quad (8)$$

As shown in Table 5, the ANN with input type III gives the best result. Fig. 3 shows the percentages of number of points in every 10% mean deviation range when the ANN result is compared with the experimental data. The abscissa gives the average deviation range such as −50% to −40%, −40% to −30%, −30% to −20%, and so on up to +40% to +50% errors. The percentages of data points falling in each of error range are shown as vertical boxes in each region. Thus it can be seen that approximately 74% of data points fall within ±20%.

Table 6 gives the prediction deviation of some generalized correlations on the basis of the present data sets. As these correlations are developed earlier and their data sets do not cover all the refrigerants used in this study, these correlations show a poor accuracy. To make a fair comparison between these correlations and the ANN model, we recorrelate these correlations on the basis of the present data sets. Table 7 gives the recorrelated correlations and the best ANN model prediction results. As we can see, the ANN model is much better than the other five generalized correlations.

Weights of the best ANN are listed in Table 8.

Table 6
Original prediction results of existing generalized correlations

Deviation (%)	Liu–Winterton [6]	Jung–Radermacher [7]	Gungor–Winterton [8]	Kandlikar [9]	Shah [10]
AD	9.4	10.9	28.1	4.7	−10.8
MD	23.4	30.4	33.2	25.5	37.2
RD	35.6	42.7	47.3	34.7	30.8

Table 7
Comparison of the best ANN and new correlated correlation result

Deviation (%)	Liu–Winterton	Jung–Radermacher	Gungor–Winterton	Kandlikar	ANN
AD	−4.1	−2.5	−3.3	−4.4	2.5
MD	22.6	26.7	24.7	20.8	13.0
RD	29.3	36.3	32.3	27.01	20.3

Table 8
Weights of the best ANN with input type III

Hidden neuron	Input neuron					Output neuron
	1	2	3	4	0 (bias)	
0 (bias)	–	–	–	–	–	−4.26580E+01
1	−8.23602E+01	1.51230E+03	2.17542E−03	4.97184E−02	−1.82770E+00	2.25870E+01
2	−3.66600E+02	−4.14810E+02	1.27400E−03	9.38080E+01	1.65590E+00	−2.09120E+00
3	9.89625E+02	−2.85630E+03	7.27220E−03	1.35894E+01	5.08190E+00	3.20670E+01
4	3.06605E+00	1.59765E+03	5.98806E−03	9.42880E−01	−4.60720E+00	−2.26440E+01
5	7.44276E+02	−1.26227E+03	1.85452E−03	3.36768E+02	1.00390E+00	3.87890E+00
6	1.76254E+02	2.35500E+03	1.35343E−02	2.63658E+00	−1.02300E+01	7.81740E+00
7	−4.81182E+03	1.64235E+04	−2.37790E−02	6.64672E+00	−1.85120E+01	9.19620E−01
8	−4.59420E+02	3.76005E+03	−5.81139E−03	−1.33786E+01	−1.51860E+01	3.16840E+01

3.2. Parameter analysis

To further compare the ANN, other generalized correlations and experimental data, parameter analysis is illustrated in Figs. 4–7.

A comparison of boiling heat transfer coefficient versus quality for the experimental data and six models is presented in Figs. 4 and 5. The experimental data in Fig. 4 are from Boissieux et al. [26]. The working fluid is R22, and the working conditions are $G = 311$ kg/(m^2 s), $T_{sat} = 27$ °C, $q = 28$ kW/m^2, $D = 9.52$ mm. The heat transfer coefficient increases up to a maximum value as the vapor quality increases to 60–80%, and then drops dramatically characterizing the "dry-out" region. Compared with other correlations, the ANN model shows a better trend. The experimental data in Fig. 5 are from Lallemand et al. [25] for R407C. The working conditions are $G = 300$ kg/(m^2 s), $T_{bub} = 9.76$ °C, $T_{dew} = 15.62$ °C, $q = 10$ kW/m^2, $D = 10.7$ mm. The heat transfer coefficients versus quality show a relatively flat trend and the ANN also shows a similar trend. In addition, from the Figs. 4 and 5, it can be seen that the ANN has a good agreement with the experiment data.

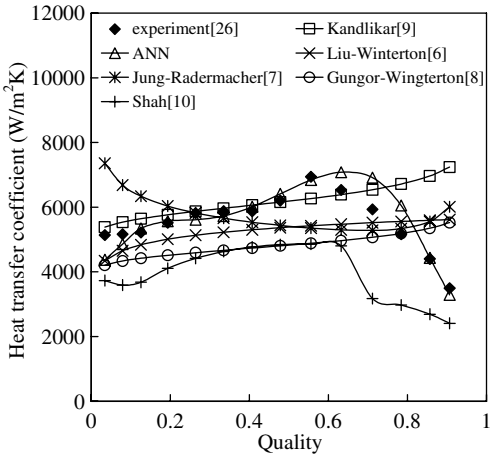

Fig. 4. Heat transfer coefficient versus quality.

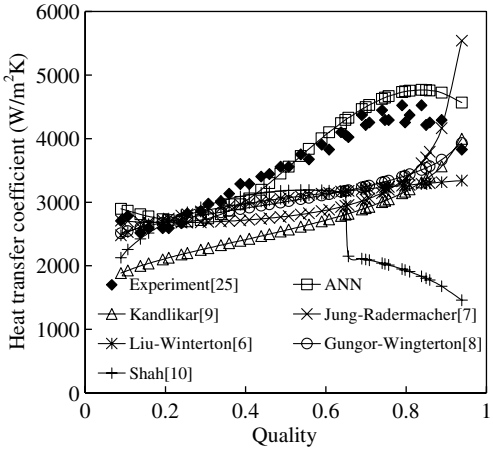

Fig. 5. Heat transfer coefficient versus quality: another case.

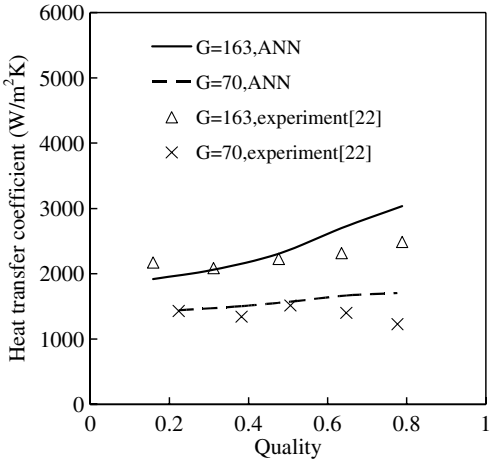

Fig. 6. Heat transfer coefficient versus quality under different mass flux.

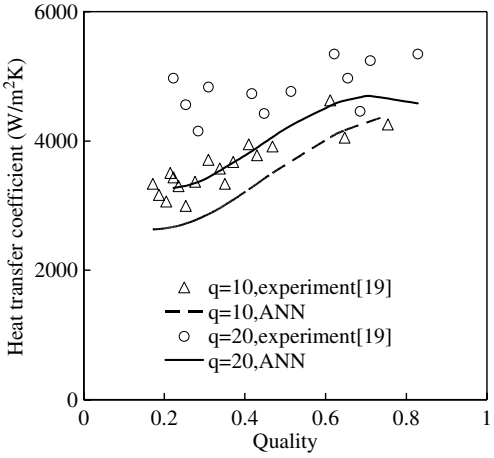

Fig. 7. Heat transfer coefficient versus quality under different heat flux.

Fig. 6 shows the trend of heat transfer coefficient versus quality under different mass flux. The experimental data are from Kim et al. [22] for R410A and the working conditions are $T_{sat} = 5$ °C, $T_{dew} = 5.098$ °C, $q = 5$ kW/m^2, $D = 8.7$ mm. In general, the heat transfer coefficient will increase with the increase of mass flux. Such a trend is shown by the experimental data as well as the ANN prediction in Fig. 6.

Fig. 7 shows the trend of heat transfer coefficient versus quality under different heat flux. The experimental data are from Wattelet et al. [19] for R134a and the working conditions are $G = 300$ kg/(m^2 s), $T_{sat} = 5$ °C, $D = 10.92$ mm. According to the experimental data, the heat transfer coefficient increases with the increase of heat flux. The ANN gives a similar trend.

From the parameter analysis above, it can be seen that the proposed ANN not only has a good agreement with experimental data but also shows a correct parametric trend among the important variables.

4. Conclusions

In this study, the neural network approach is developed to predict heat transfer coefficients of R22, R407C, R410A, and R134a flow boiling inside horizontal smooth tubes. The input of network is selected from the existing generalized correlations and compared with each other to determine the best. The transfer function and number of hidden neurons are determined by the performance of model accuracy and the standard sensitivity analysis. As a result, a three-layer perceptron of neurons 4-8-1 and using log-sig and log-sig combination as hidden and output layer transfer function is finally recommended. Compared with the experimental data, the average, mean and root-mean-square deviations of the trained neural network are 2.5%, 13.0% and 20.3%, respectively, and approximately 74% of the deviations are within ±20%, which is much better than that of the existing generalized correlations. This study shows that the neural network approach is effective in the correlation and estimation of heat transfer coefficient and promising as an alternative of the traditional correlations.

References

[1] World Meteorological Organization, Montreal protocol on substances that deplete the ozone layer report, WMO Bull 37 (1988) 94–97.

[2] World Meteorological Organization, Scientific assessment of ozone depletion: 1994. WMO Global Ozone Research and Monitoring Project Report Geneva 37, 1995.

[3] J.R. Thome, Boiling of new refrigerants: a state-of-the-art review, Int. J. Refrig. 19 (7) (1996) 435–457.

[4] J. Darabi, M. Salehi, M.H. Saeedi, M.M. Ohadi, Review of available correlations for prediction of flow boiling heat transfer in smooth and augmented tubes, ASHRAE Trans. 101 (1) (1995) 965–975.

[5] M.P. Mishra, H.K. Varma, C.P. Aharma, Heat transfer coefficients in forced convection evaporation of refrigerants mixtures, Lett. Heat Mass Transfer 8 (2) (1981) 127–136.

[6] Z. Liu, R.H.S. Winterton, A general correlation for saturated and subcooled flow boiling in tubes and annuli based on a nucleate pool boiling, Int. J. Heat Mass Transfer 34 (1991) 2759–2765.

[7] D. Jung, R. Radermacher, Transport properties and surface tension of pure and mixed refrigerants, ASHRAE Trans. 97 (1991) 90–99.

[8] K.E. Gungor, R.H.S. Winterton, A general correlation for flow boiling in tubes and annuli, Int. J. Heat Mass Transfer 29 (1986) 351–358.

[9] S.G. Kandlikar, A general correlation for saturated two-phase flow boiling heat transfer inside horizontal and vertical tubes, ASME J. Heat Transfer 112 (1990) 219–228.

[10] M.M. Shah, Chart correlation for saturated boiling heat transfer: Equations and farther study, ASHRAE Trans. 88 (1) (1982) 185–196.

[11] T.Y. Choi, Y.J. Kim, M.S. Kim, S.T. Ro, Evaporation heat transfer of R-32, R-134a, R-32/134a, and R-32/125/134a inside a horizontal smooth tube, Int. J. Heat Mass Transfer 43 (2000) 3651–3660.

[12] S.S. Sablani, A neural network approach for non-iterative calculation of heat transfer coefficient in fluid–particle systems, Chem. Eng. Process. 40 (4) (2001) 363–369.

[13] K. Jambunathan, S.L. Hartle, S. Ashforth-Frost, V.N. Fontama, et al., Evaluating convective heat transfer coefficients using neural network, Int. J. Heat Mass Transfer 39 (1996) 2329–2332.

[14] G. Scalabrin, L. Piazza, Analysis of forced convection heat transfer to supercritical carbon dioxide inside tubes using neural networks, Int. J. Heat Mass Transfer 46 (2003) 1139–1154.

[15] Y. Islamoglu, A new approach for the prediction of the heat transfer rate of the wire-on-tube type heat exchanger—use of an artificial neural network model, Appl. Therm. Eng. 23 (2003) 243–249.

[16] C.C. Wang, C.S. Chiang, Two-phase heat transfer characteristics for R22/R407C in a 6.5 mm smooth tube, Int. J. Heat Fluid Flow 18 (1997) 550–558.

[17] K. Seo, Y. Kim, Evaporation heat transfer and pressure drop of R22 in 7 and 9.52 mm smooth/micro-fin tubes, Int. J. Heat Mass Transfer 43 (2000) 2869–2882.

[18] A. Muzzio, A. Niro, S. Arosio, Heat transfer and pressure drop during evaporation and condensation of R22 inside 9.52 mm O.D. micro-fin tube of different geometries, Enhanced Heat Transfer 5 (1998) 39–52.

[19] J.P. Wattelet, J.C. Chato, A.L. Souza, B.R. Christoffersen, Evaporative characteristics of R12, R134a, and a mixture at low mass fluxes, ASHRAE Trans. 100 (1) (1994) 603–615.

[20] L. Zhang, H. Eiji, S. Takamoto, Boiling heat transfer of a ternary refrigerant mixture inside a horizontal smooth tube, Int. J Heat Mass Transfer 40 (9) (1997) 2009–2017.

[21] C.C. Wang, C.S. Kuo, Y.J. Chang, D.C. Lu, Two-phase flow heat transfer and friction characteristics of R-22 and R407C, ASHRAE Trans. 102 (1) (1996) 830–838.

[22] Y. Kim, K. Seo, J.T. Chung, Evaporation heat transfer characteristics of R410A in 7 and 9.52 mm smooth/micro-fin tubes, Int. J. Refrig. 25 (6) (2002) 716–730.

[23] T. Ebisu, K. Torikoshi, Heat transfer characteristics and correlations for R410A flowing inside a horizontal smooth tube, ASHRAE Trans. 104 (2) (1998) 556–561.

[24] J.Y. Shin, M.S. Kim, S.T. Ro, Experimental study on forced convective boiling heat transfer of pure refrigerants and refrigerant mixtures in a horizontal tube, Int. J. Refrig. 20 (4) (1997) 267–275.

[25] M. Lallemand, C. Branescu, P. Haberschill, Local heat transfer coefficients during boiling of R22 and R407C in horizontal smooth and microfin tubes, Int. J. Refrig. 24 (1) (2001) 57–72.

[26] S. Boissieux, M.R. Heikal, R.A. Johns, Two-phase heat transfer coefficients of three HFC refrigerants inside a horizontal smooth tube, part I: evaporation, Int. J. Refrig. 23 (4) (2000) 269–283.

[27] W. Huang, S. Foo, Neural network modeling of salinity variation in Apalachicola River, Water Res. 36 (2002) 356–362.

[28] G. Cybenko, Approximation by superpositions of a sigmoidal function, Math. Control Signals Syst. 2 (1989) 303–314.

[29] K. Hornik, M. Stinchcombe, H. White, Multilayer feedforward networks are universal approximators, Neural Networks 2 (1989) 359–366.

[30] V. Kurkova, Kolmogorov's theorem and multilayer neural networks, Neural Networks 5 (1992) 501–506.

[31] Y. Ito, Approximation capabilities of layered neural networks with sigmoid units on two layers, Neural Comput. 6 (1994) 1233–1243.

[32] M. Aydinalp, V.I. Ugursal, A.S. Fung, Predicting residential appliance, lighting, and space cooling energy consumption using neural networks, in: Proceedings of the Fourth International Thermal Energy Congress, Turkey, 2001.

[33] A. Greco A, G.P. Vanoli, Flow boiling heat transfer with HFC mixtures in a smooth horizontal tube. Part II: Assessment of predictive methods, Exp. Therm. Fluid Sci. (2004) 1–10.

[34] F. Lefevre, C. Le Niliot, A parameter estimation approach to solve the inverse problem of point heat sources identification, Int. J. Heat Mass Transfer 47 (2004) 827–841.